Romanian Reports in Physics, Vol. 64, No. 2, P. 436–445, 2012

BIOPHYSICS

A SIMPLE EVALUATION OF THE RESIDUAL RADIOACTIVITY INDUCED IN A TCP BONE GRAFT SUBSTITUTE, FOLLOWING A HADRON THERAPY PROCEDURE

LIGIA PALADE[1], GH. CATA-DANIL[2]

[1] "Politehnica" University of Bucharest, Physics Department, Romania
E-mail: ligia.palade@yahoo.com
[2] "Politehnica" University of Bucharest and "Horia Hulubei" National Institute for Physics and Nuclear Engineering, Physics Department, Magurele, Romania

Received August 22, 2011

Abstract. In the present study it is evaluated, in a simplified model, the residual radioactivity following a hadrons therapy treatment, in a very specific situation. The specificity of this work refers to the case when a part of the incident ^{12}C and proton beams hits a bone graft substitute made from tricalcium phosphate (TCP) compound, located in a region near the Bragg Peak. Realistic beams energies and irradiation geometry are embedded in an analytic traceable model. Specific radioactivity of TCP is evaluated at the end of the irradiation period and several time intervals later, up to one hour. The information is in many respects complementary to that obtained by the standard radiation transport codes and is valuable for precise dosimetry in treatment planning.

Key words: protons and heavy ions radiotherapy, tricalcium phosphate, residual specific activity, nuclear reactions.

1. INTRODUCTION

The use of protons and heavy-ions beams in cancer treatment allows an accurate irradiation of tumors with minimum impact on healthy tissues. For both beams, a residual radioactivity of the irradiated tissue occurs due to nuclear reactions induced along the beams trajectory. In the present work we performed an estimation of residual specific activity at the end of irradiation and its time evolution over one hour. The irradiation model considers a bone graft substitute, tricalcium phosphate (TCP) based material, located near a tumor. The tumor is irradiated with proton and carbon-ion beams. Some of the ions from the incident beams will bombard this substitute bone graft producing nuclear reactions with its atomic nuclei. The energies considered for the incident beams are 50 MeV for the protons and 100 MeV for carbon-ions beams. These energies are reached in the real treatments, by the bombarding hadrons beams, in a region located before the peak region of the Bragg curve.

2. USE OF THE HADRONS BEAMS IN MEDICAL THERAPY

Radiotherapy techniques use the ionizing radiation to kill cancer cells by damaging their genetic material, and reducing tumors size. High energy photon and electron beams are extensively used nowadays, targeting the tumor from different directions in order to minimize the doses in the healthy tissues. These techniques are called "conventional" radiotherapy [1–2].

An accurate irradiation of tumors with minimum impact on healthy tissues becomes possible by using proton and heavy ions [3]. The procedure has been proposed for the first time in 1946 by Wilson *et al.* [4]. Such projectiles deliver enhanced dose at the very end of their range, as reflected in their stopping power curve shape (Bragg curve – see for example Fig.1). This innovative technique (proton and heavy-ion radiotherapy or hadrons therapy), opens the possibility of a precise dose deposition in a well defined region of the body (in deep-seated tumors), by an accurate irradiation planning. The irradiation plan in this kind of therapy relies heavily on numerical simulations of the heavy ion stopping in biological tissues, by deterministic or Monte Carlo methods.

Heavy ion beams add more physical and biological advantages for effective cancer therapy compared even with proton beams. For carbon beams, important advantages are the higher linear energy transfer (LET) a reduced longitudinal and lateral scattering in tissues and a much higher relative biological effectiveness (see for example Ref. [6]).

For both proton and carbon ion beams a residual radioactivity of the irradiated tissue occurs due to induced nuclear reactions, along the trajectory. This is a physical side effect of the irradiation which should be considered for detailed dosimetric planning in these modern therapy techniques.

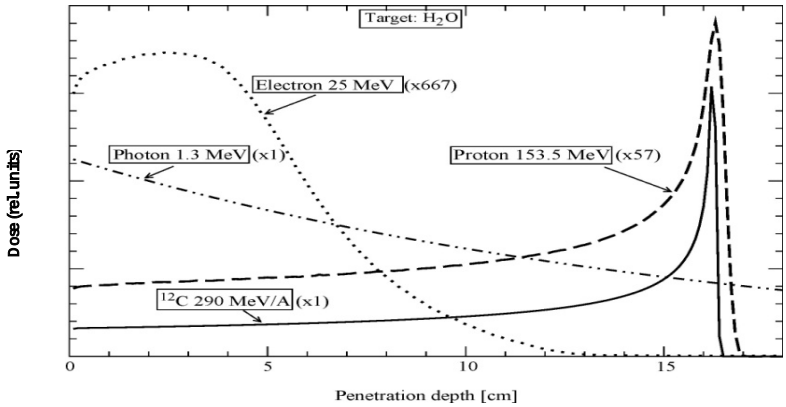

Fig. 1 – Relative dose deposited in a thick target of water as a function of the penetration depth by several types of radiations employed in radiotherapy. The simulations have been performed with the computer code FLUKA. Data are taken from Ref. [5].

3. TRICALCIUM PHOSPHATE, A COMPOUND OF THE BONE GRAFT SUBSTITUTES

There are situations in which bone grafts substitutes are used to fill voids and support biologic repair of skeletal defects. Bone substitute with osteoconductive properties act as a framework allowing the native bone to grow onto and form the new bone [7]. Many modern synthetic bone graft substitutes contain tricalcium phosphate (TCP) bioceramic, a compound with chemical formula $Ca_3(PO4)_2$. TCP is a variety of hydroxyapatite with a modified structure and a proportion of calcium and phosphorus, similar to that of the bone. Because of the good bioresorbability and low complication rate, TCP is a suitable material for medical applications, *e.g.* the filling of bone defects or coating to promote bone ingrowths into prosthetic implants [8].

During radiotherapy these non-biological materials are subject to ionization radiation fields. A question arises about their "radioactive response" following the irradiation. In the present work we have imagined a scenario of a tumor located at a small distance of a synthetic bone graft substitute (TCP based material) and irradiated with high energy hadrons beam. The aim of our study is to evaluate the residual radioactivity induced by irradiation of proton and carbon ions in this TCP based bone substitute. The residual specific activity of the TCP compound and the time evolution of the activity following the hadrons irradiation has a potential impact on the accurate dosimetric evaluation reflected by treatment plan. From our knowledge it is for the first time when such a problem is tackled and there are few published works on this subject, none of them referring to hadrons irradiation (*e.g.* Ref [9]).

4. THE IRRADIATION MODEL EMPLOYED IN THE PRESENT WORK

4.1. ASSUMPTIONS ON MATERIALS AND GEOMETRY OF IRRADIATION

As we mentioned above, we consider a situation in which a tumor is treated with a high energy hadrons beam. There can be situations in which near the end of the ions beam trajectory in the body (Bragg peak area) there is located a synthetic substitute bone graft. In such a scenario, some of the ions will bombard this substitute TCP based material (with chemical formula: $Ca_3(PO_4)_2$), producing nuclear reaction on the calcium, oxygen and phosphor ions. It is the goal of the present paper to explore the residual specific activity produced in this material, after the irradiation with protons and carbon beams. Both the types of produced radionuclides and their activities are of interest.

In our model we assume that the tumor with a nearby TCP implant is irradiated with a beam of carbon ions of 100 MeV and with a beam of protons of 50 MeV. At these bombarding energies the dominant reaction mechanism is the

compound nucleus [10]. These energies are reached by the bombarding hadrons beams before the peak region of the Bragg curve. Therefore, the radioactivity estimations in the present work are specific for this region. In order to calculate the residual specific activity following irradiation process and its time-evolution, we used an irradiation model including ions beams of 5 mm diameter (as given for example in refs. [11–12]) and a beam intensity level considered to be equal to 10^9 pps [13], bombarding the target for five minutes.

We assumed that the TCP layer is thin and therefore the decrease of beam energy on it can be neglected. This is a realistic assumption since many modern implants are just coated with TCP. We have also assumed that the radionuclides resulting from the nuclear reaction do not generate at their turn other nuclear reactions. The density considered for the TCP-sample is 3.14g/cm^3 and the molar mass is 310.18 g/mol.

4.2. CROSS SECTIONS USED IN REACTION RATES ESTIMATIONS

In order to get a realistic estimation of the activity besides the tissues and beam characteristics there are needed absolute cross sections for all possible nuclear reactions occurring between the beam particles and the nuclei from the substitute tissue. Experimental values of the cross sections (when measured) are taken in the present study from Ref. [14]. Whenever experimental data are not known we relayed on the statistical model calculations. The computer code PACE4 [15] was employed to estimate the relative values for the needed cross sections. The calculated values were normalized to the experimental one whenever available.

As mentioned before, at the bombarding energies used in our study the dominant reaction mechanism is compound nucleus. The partial cross section for the formation of a compound nucleus state of spin J and parity Π, from a projectile and a target nucleus of spins J_p and J_T respectively, at centre of mass energy E is given, (as discussed *e.g.* in ref. [16]), by:

$$\sigma(J,\Pi) = \pi\lambda^2 \frac{2J+1}{(2J_p+1)(2J_T+1)} \sum_{S=|J_p-J_T|}^{J_p+J_T} \sum_{L=|J-S|}^{J+S} T_L(E), \qquad (1)$$

where: T_L are the transmission coefficients dependent on energy, L is the orbital angular momentum, and S (= J_p+J_T) is the channel spin.

The transmission coefficients are derived by using optical model parameters for inverse fusion reactions. The optical model parameters are taken from the systematics (*e.g.* RIPL [17]). The total fusion cross section for the formation of the compound nucleus is given [16], by:

$$\sigma = \pi\lambda^2 \sum_{L=0}^{L_c} (2L+1) T_L(E), \qquad (2)$$

where L_c is the maximum angular momentum transferred to the compound system.

The decay probabilities are determined by the level densities of the daughter nuclei and the barrier penetrability's for various channels. The Gilbert and Cameron formalism is used in order to estimate the level densities value [15].

5. TIME EVOLUTION OF THE TCP TISSUE-LIKE ACTIVITY FOLLOWING HADRONS IRRADIATION

5.1. CARBON IONS BEAM IRRADIATION

As mentioned above, we calculated the residual specific activity produced in a TCP bone substitute after irradiation with a 100 MeV carbon ions beam. The beam, with the characteristics given in section 4.1, bombards the TCP target for five minutes, a time length comparable with the one used in real treatments. In order to calculate the residual specific activity $\Lambda_{0,}$ due to a radionuclide with the decay constant λ, following a irradiation process, we employed the standard relation [18]:

$$\Lambda_0 = \Sigma\, \Phi\, (1–\exp\,(–\lambda \Delta t)), \tag{3}$$

where Σ is the total macroscopic cross section for formation of the considered radionuclide, Φ is the incident particle flux and Δt is the irradiation time.

Half lifes for the radio nuclides are taken from Ref. [14]. The results of the calculations are given in the Fig. 2. At the end of the irradiation process the total specific activity is 1 006.3 μCi, a significant value from a dosimetric perspective. In order to estimate the later effects of the irradiation we have calculated the time-evolution of residual specific activity at each five minutes over one hour long, by using the exponential decay law for each radionuclide. We notice a significant decrease of the residual total specific activity in the first five minutes following the end of the irradiation process. The activity after five minutes is 115.8 μCi, 11.51% from initial activity. This fast initial decrease, is followed by a slight decrease as shown in Fig. 2, with small steps (from 23.5 to 2.5 μCi) at each five minutes and, after one hour, the specific activity becomes 34.5 μCi.

An important part of the total specific residual activity, at the end of the irradiation process, is produced by the ^{21}Na, ^{25}Al and ^{15}O radionuclides. Their residual specific activity is 285 μCi, 207 μCi and 197 μCi respectively. There are also others relevant nuclides, with important contribution to the total specific activity, as: ^{42}Sc, ^{47}V, ^{30}P, ^{38}K, ^{26}Al (with values between 20 and 90 μCi). Their contribution to the total specific residual activity at the end of the irradiation is 289 μCi.

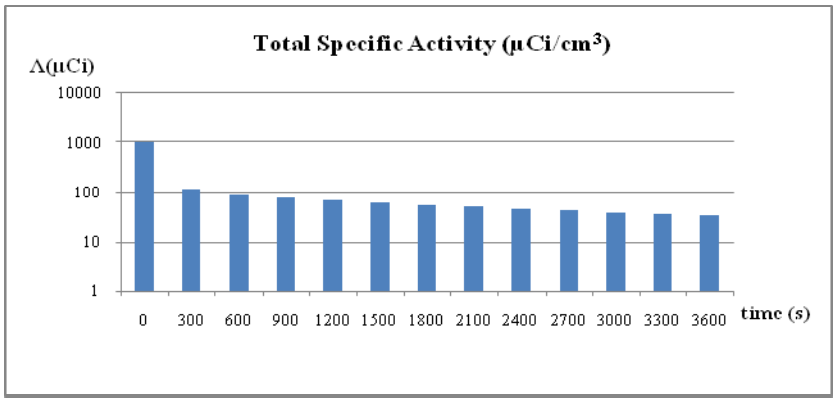

Fig. 2 – Time evolution of the total residual specific activity during one hour, after the irradiation with carbon ions beam (see text for details). Time 0 refers to the moment when irradiation is stopped.

In the Table 1 are presented the specific activities and cross sections of the long half-lives radionuclides ($T_{1/2}$ days and years) at the end of the irradiation time. The total residual specific activity at the end of the irradiation is 642,8 nCi, and an important part of it, is given by the ^{44}Sc nuclide (about 558 nCi).

Table 1

The specific activities and the formation cross sections of the long half-lives radionuclides ($T_{1/2}$ days and years) at the end of the irradiation time

No	Nuclides	Half-life*	σ (mb)**	A_0 (n Ci)**
1	44 Ti	60 a	82.5	0.023
2	55 Fe	2.73 a	92.1	0.001
3	22 Na	2.602 a	92.5/30.3/122.6	1.582
4	49 V	331 d	231.6/69.8/205.5/261.2	0.059
5	54 Mn	312.10 d	364.0	0.013
6	35 S	87.51 d	69.7	3.216
7	46 Sc	83.81 d	63.7/30.6/26.1	0.033
8	37 Ar	35.04 d	56.8	6.546
9	51 Cr	27.702 d	275.2/325.7/29.1/79.4	1.399
10	33 P	25.34 d	31.3	4.998
11	48 V	15.974 d	67.4/289.1/203.8/68.8	27.609
12	32 P	14.262 d	138.3	39.169
13	52 Mn	5.591 d	254.3	0.011
14	47 Sc	3.360 d	28.9/66.4	0.075
15	44 Sc	58.6 h	231.6/47.0/89.9	558.104

*Half-lives for the nuclides in the table above are taken from Ref. [14].

**See text for details on the calculations of cross sections and total specific activity at the end of the irradiation time. The lines with multiple cross sections values comes from nuclear reactions of the incident beam with several stable isotopes contained in TCP target. Natural abundances have been considered in activities estimations for all cases.

A part of radionuclides produced by bombarding the TCP bioceramic with carbon ion beam are positron emitters. Table 2 presents the activities and cross sections of these nuclides. Positron emitters can be used in PET (Positron Emission Tomography) techniques, for the real-time dose distribution monitoring during irradiation.

Table 2

The relevant specific activity and cross section of the positron emitters radionuclides produced by bombarding the TCP bioceramic with carbon ion beam

No	Nuclides	Half-life*	σ (mb)**	Λ_0 (n Ci)**
1	21 Na	22.48 s	42.5	284674.632
2	25 Al	7.183 s	30.8	206525.663
3	15 O	2.037 m	35.9	196498.049
4	42 Sc	61.7 s	38.3	90327.036
5	47 V	32.6 m	310.0/91.9	76805.706
6	30 P	2.498 m	28.9	36415.733
7	38 K	7.64 m	57.5/34.5	65882.836
8	26 Al	6.345 s	146.5	20163.741
9	44 Sc	3.927 h	231.6	8255.697
10	45 Ti	3.080 h	133.4	6050.139
11	43 Sc	3.891 h	47.9	1722.681
12	51 Mn	46.3 m	119.8	453.901
13	49 Cr	42.2 m	252.5	324.351

*Half-lives for the nuclides in the table above are taken from Ref. [14].

**See text for details on the calculations of cross sections and total specific activity at the end of the irradiation time. The lines with multiple cross sections values comes from nuclear reactions of the incident beam with several stable isotopes contained in TCP target. Natural abundances have been considered in activities estimations for all cases.

The largest specific activity, as shown in the Table 2, is produced by ^{21}Na, ^{25}Al and ^{15}O radionuclides.

5.2. PROTONS BEAM IRRADIATION

In many cases in tumor irradiation therapy the proton ions beam are also successfully employed. When in the model described in the previous section, the carbon ions beam is replaced with the proton beam, the total specific residual activity after five minutes of irradiation is 273.6 μCi. An important part (125.6 μCi) is due to ^{38}K radionuclide.

The time-evolution of specific residual activity (each five minutes, over one hour) for the proton beam is presented in Fig. 3. In this case, after five minutes

following the irradiation process, the residual specific activity is 79.8 μCi. The initial fast decreasing component is 193.8 μCi. This is followed by a slow decrease of the specific residual activity, in the range 29.1–0.3 μCi.

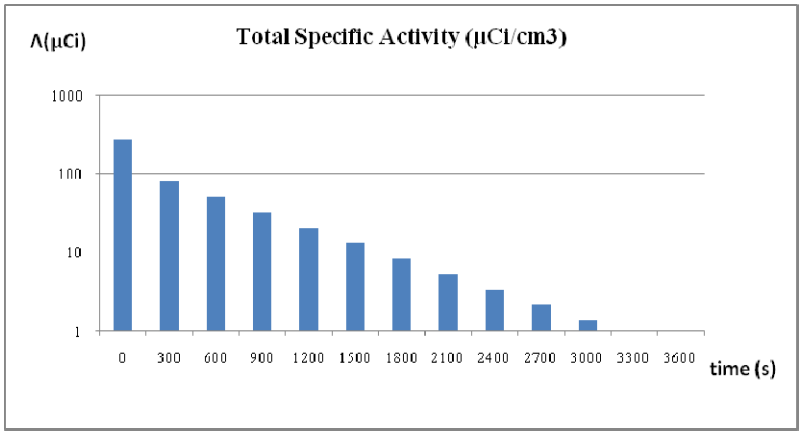

Fig. 3 – Time evolution of the total residual specific activity during one hour after the irradiation with proton beam (see text for details). Time 0 refers to the moment when irradiation is stopped.

The specific activities and cross sections of the long half-lived radionuclides ($T_{1/2}$ days and years) at the end of the irradiation time are presented in the Table 3. The total residual specific activity at the end of irradiation process is 20.9 nCi, and the most important contribution is given by ^{37}Ar nuclide.

Table 3

The specific activities and cross sections of the long half-lives radionuclides ($T_{1/2}$ days and years) at the end of the irradiation time

No	Nuclides	Half-life*	σ (mb)**	A_0 (n Ci)**
1	45 Ca	162.7 d	244.9	0.017
2	46 Sc	83.81 d	112.5	0.015
3	37 Ar	35.04 d	122.8/200.0/111.9	20.832
4	44 Sc	58.6 h	138.5	0.014

*Half-lives for the nuclides in the table above are taken from Ref [14].

**See text for details on the calculations of cross sections and total specific activity at the end of the irradiation time. The lines with multiple cross sections values comes from nuclear reactions of the incident beam with several stable isotopes contained in TCP target. Natural abundances have been considered in activities estimations for all cases.

The residual specific activities and production cross sections of the positron emitters, in the case of the proton beam irradiations, are given in Table 4.

Table 4

The specific activities and cross sections of the positron emitters radionuclides produced by bombarding the TCP bioceramic with carbon ion beam

No	Nuclides	Half-life*	β	σ (mb)**	Λ_0 (n Ci)**
1	44 Sc	3.927 h	β^+	138.5	0.203
2	43 Sc	3.891 h	β^+	91.7	0.136
3	38 K	7.64 m	β^+	141/49	125611.147
4	26 Al	6.345 s	β^+	87.8	147460.3

*Half-lives for the nuclides in the table above are taken from Ref. [14].

**See text for details on the calculations of cross sections and total specific activity at the end of the irradiation time. The lines with multiple cross sections values comes from nuclear reactions of the incident beam with several stable isotopes contained in TCP target. Natural abundances have been considered in activities estimations for all cases.

In this case, by far the largest radioactivity is due to the ^{38}K radionuclide, with 7.64 minutes half life.

6. CONCLUSIONS AND PERSPECTIVES

The decision to use either carbon or proton beams in the radiotherapy of cancer treatment should balance their specific advantages and disadvantages. One parameter to be considered is the induced radioactivity following the irradiation procedure. In the present work a specific situation has been considered. It refers to a "side-irradiation" of a TCP based bone substitute located near the tumor in the Bragg peak region. For the case of the treatment with ^{12}C beams we have estimated a specific activity of 1 006.3 μCi at the end of the irradiation process. We notice a sharp decrease after five minutes from the end of the irradiation process, at 115.8 μCi. The estimation of the time-evolution of residual specific activity at each five minutes over one hour time interval shows that this initial fast decrease is followed by a slight decrease, with small values (23.5–2.5 μCi) and, after one hour, the specific activity decrease to 34.5 μCi.

When the proton beams are employed in our model, the total specific activity at the final of the irradiation time is 273.6 μCi, 3.7 times smaller than in the case of the carbon-ion beam with the same particle flux. The initial residual specific activity decreases at 79.8 μCi after five minutes from the end of the irradiation process. This is followed by a slow decrease of the specific residual activity, in the range of 29.1–0.3 μCi.

The present schematic model (analytical) must be followed by complete Monte Carlo simulations. These studies are needed for accurate dosimetric planning of radiotherapy with hadrons beams.

REFERENCES

1. H. E. Johns and J. R. Cunningham, *The Physics of Radiology*, Fourth Edition, C. C. Thomas Publisher, Springfield, IL, 1983.
2. J. J. Bevelacqua, *Contemporary Health Physics*, Problems and Solutions, John Wiley & Sons, Inc., New York, 1995.
3. G. Kraft, *Tumor Therapy with Heavy Charged Particles*, Progress in Particle and Nuclear Physics, **45**, S473, 2000.
4. R.R. Wilson, *Radiological use of fast protons*, Radiology, **47**, 487–491, 1946.
5. J. Soltani-Nabipour, Gh Cata-Danil, *Monte Carlo computation of the energy deposited by heavy charged particles in soft and hard tissues,* U.P.B. Sci. Bull., Series A, **70**, *3*, 2008.
6. William T. Chu, *Heavy Ion Radiotherapy: Yesterday, Today and Tomorrow*, Proc. of 10th Heavy Ion Charged Particle Therapy Symposium, International Symposium on Heavy Ion Radiotherapy and Advanced Technology, National Institute of Radiological Sciences Japan, 12–13 January, 2011.
7. Giuliano Gregori, Hans-Joachim Kleebe, Helmar Mayra, Gunter Ziegler*, EELS characterisation of β-tricalcium phosphate and hydroxyapatite*, Journal of the European Ceramic Society, **26**, pp. 1473–1479, 2006.
8. Stephen Kantor Leonard Rosenthall, J.Dennis Bobyn, *Femoral remodeling after porous-coated total hip arthroplasty with and without hydroxyapatite-tricalcium phosphate coating*, The Journal of Arthroplasty, **16**, pp. 552–558, 2000.
9. W. G. Osiris, Wafa I. Abdel-Fattah, Z. Mohsen & A. El-Shabini*, Bone and tricalcium phosphate bioceramic response to low level fast neutron irradiation*, Radiation Effects and Defects in Solids, **140**, *3–4*, pp. 385–394, 1997.
10. P. E. Hodgson, E. Gadioli, E. Ggadioli Erba, *Introductory Nuclear Physics*, Oxford Science Publications, New York, 1997.
11. D.V.A. Babkin, G. Cata-Danil, V.M. Golovatyuk, G. Moloknov, M.M. Paraipan, G.N. Timoshenko, *SOBP forming for carbon therapy*, Central Eur. J. of Phys., **8**, *4*, pp. 683–688, 2010.
12. Paraipan M., Sobolevsky N., Timoshenko G., Florko B.*, Verification of Monte Carlo transport codes Fluka and Geant for radiation protection purposes at relativistic heavy ion accelerator*, Nucl. Instr. And Meth. In Phys. Res. B, **266**, pp. 4058–4062, 2008.
13. *** http://www.nirs.go.jp/ENG/publications/pdf/proceedings_e.pdf
14. *** http://www.nndc.bnl.gov/
15. A. Gavron, *Statistical model calculations in heavy ion reactions*, Phys. Rev C, **21**, *1*, pp. 230–236, 1980.
16. A. Mihailescu, Gh. Cata-Danil, *Gamma-ray production in the 58 Ni(16O,X*), Rom. Journ. Phys., **55**, *7–8*, pp. 712–723, 2010.
17. *** http://www-nds.iaea.org/ripl2/
18. F.H. Attix *Introduction to Radiological Physics and Radiation Dosimetry*, John Willey and Sons, Inc., 1986.